Circulation: Cardiovascular Interventions

ORIGINAL ARTICLE

Three-Dimensional CT for Preprocedural Planning of PCI for Ostial Right Coronary Artery Lesions: A Randomized Controlled Pilot Trial

Deborah M.F. van den Buijs, MD; Ella M. Poels, MD, PhD; Endry Willems, MD; Daan Cottens, MD; Kevin Dotremont, MSc; Karen De Leener, MSc; Evelyne Meekers, MD; Bert Ferdinande, MD; Mathias Vrolix, MD; Joseph Dens, MD, PhD; Koen Ameloot, MD

BACKGROUND: Geographic stent-ostium mismatch is an important predictor of target lesion failure after percutaneous coronary intervention of an aorto-ostial right coronary artery lesion. Optimal visualization of the aorto-ostial plane is crucial for precise stent implantation at the level of the ostium. This study investigates whether preprocedural 3-dimensional computed tomography (3DCT), with determination of the optimal viewing angle, would allow for more precise stent implantation and reduce procedure time, contrast, and radiation dose.

METHODS: In this single-center, prospective, open-label, core-laboratory blinded trial, a total of 30 patients with an aorto-ostial right coronary artery lesion were randomly assigned to either percutaneous coronary intervention with a preprocedural 3DCT or angiography-guided percutaneous coronary intervention. The optimal working view angle was determined by 3DCT in the intervention group and by the operators' discretion in the control group. The primary end point was the percentage of patients without geographic mismatch, as determined by intravascular ultrasound.

RESULTS: 3DCT-determined C-arm angles were heterogenous but, in general, more extreme left anterior oblique projections were used ($P<0.0001$). While stent implantation was in the optimal position in all patients randomized to the intervention group, geographic mismatch was present in 5 (33%) patients randomized to the control group ($P=0.06$). The mean amount of procedural contrast ($P<0.0001$), mean radiation ($P=0.03$), and median procedure time ($P=0.03$) were significantly lower in the intervention group. The 3DCT scan was able to predict the calcium arc ($P<0.0001$) and minimal lumen area by intravascular ultrasound ($P=0.003$).

CONCLUSIONS: Preprocedural 3DCT planning for percutaneous coronary intervention of aorto-ostial right coronary artery lesions allows for optimal stent positioning while reducing procedure time, contrast, and radiation dose.

REGISTRATION: URL: https://www.clinicaltrials.gov; Unique identifier: NCT05172323.

GRAPHIC ABSTRACT: A graphic abstract is available for this article.

Key Words: angiography ■ control groups ■ coronary vessels ■ humans ■ percutaneous coronary intervention

Even with contemporary drug-eluting stents and calcium modification strategies, percutaneous coronary intervention (PCI) of an ostial right coronary artery (RCA) lesion remains associated with a 4.49% rate of target lesion failure at 1 year and a 14.2% rate of target lesion revascularization (TLR) at 3 years.[1–9]

Specific anatomic characteristics of the aorto-ostial RCA area may contribute to higher rates of TLR such as the funnel-shaped morphology and the tendency to recoil due to the greater amount of muscular and elastic tissue in the adjacent aortic wall.[10,11] Furthermore, extensive calcification may result in stent underexpansion[12,13]

Correspondence to: Deborah M.F. van den Buijs, MD, Ziekenhuis Oost-Limburg, Synaps Park 1, 3600 Genk, Belgium. Email d.vandenbuijs@gmail.com
Supplemental Material is available at https://www.ahajournals.org/doi/suppl/10.1161/CIRCINTERVENTIONS.123.013584.
For Sources of Funding and Disclosures, see page 112.

Circulation: Cardiovascular Interventions is available at www.ahajournals.org/journal/circinterventions

WHAT IS KNOWN

- Even with drug-eluting stents, calcium modification strategies, and different techniques to optimize stent positioning, percutaneous coronary intervention of an ostial right coronary artery lesion is associated with a target lesion revascularization of 14.2% at 3 years.

WHAT THE STUDY ADDS

- The addition of preprocedural 3-dimensional computed tomography with determination of the optimal viewing angle during percutaneous coronary intervention allows for better stent positioning while reducing procedure time, contrast, and radiation dose.
- Further research is warranted to evaluate the addition of preprocedural 3-dimensional computed tomography for percutaneous coronary intervention of an ostial right coronary artery lesion to reduce target lesion revascularization.
- Furthermore, its value in percutaneous coronary intervention of bifurcation lesions remains to be investigated.

Nonstandard Abbreviations and Acronyms

3DCT	3-dimensional computed tomography
CT	computed tomography
IVUS	intravascular ultrasound
LAO	left anterior oblique
MLA	minimal lumen area
PCI	percutaneous coronary intervention
RCA	right coronary artery
TLR	target lesion revascularization

and contact of the guide catheter with the proximal protruding stent may result in longitudinal stent compression.[8] Importantly, PCI of ostial lesions is associated with geographic mismatch in up to 50% of patients.[5,14,15] Protruding stent struts can result in increased platelet activation, thrombus formation, and distal embolization, making future procedures more challenging because of difficulty in catheter reengagement of the coronary ostium.[8,16] Conversely, a too distal implantation of the stent increases the risk of restenosis by leaving part of the lesion uncovered by stent struts.

Accurate visualization of the aorto-ostial plane is crucial to minimize foreshortening or overlap. Retrospective studies have demonstrated that a significant amount of unrecognized vessel foreshortening occurs in the working views selected by experienced interventional cardiologists.[17,18] In a previous retrospective computed tomography (CT) study, the average optimal viewing angle for PCI of aorto-ostial RCA lesions was left anterior oblique (LAO) 79° and cranial (CRA) 41°.[17] However, because there may be significant anatomic heterogeneity between patients, we hypothesize that individualized preprocedural 3-dimensional CT (3DCT) based determination of the optimal viewing angle could prevent geographic mismatch and avoid unnecessary contrast agent use and radiation during PCI. Secondarily, we also aim to investigate whether a preprocedural 3DCT may predict lesion characteristics such as the calcium arc, minimal lumen area (MLA), and vessel diameter (mm).

METHODS

Study Design

In this single-center, prospective, open-label, core-laboratory blinded trial, a total of 30 patients with an aorto-ostial RCA lesion were randomly assigned to either PCI with a preprocedural 3DCT (intervention group) or angiography-guided PCI (control group). An ostial RCA lesion was defined as a >70% angiographic stenosis within 5 mm of the origin of the ostium. Exclusion criteria were an emergent PCI indication, in-stent restenosis or thrombosis, renal insufficiency (estimated glomerular filtration rate <30 mL/min), or a known allergic reaction to contrast medium. Written informed consent was obtained before inclusion in the trial. Eligible patients were randomized in a 1:1 ratio by means of an online module (Castor Electronic Data Capture), as stratified by whether advanced calcium modification strategies, such as rotablator or laser atherectomy, were anticipated. All procedures were performed by 6 different interventional cardiologists at Ziekenhuis Oost-Limburg, Genk, Belgium. The trial was approved by the ethics committee (Z-2021107) and registered at https://www.clinicaltrials.gov (Unique identifier: NCT05172323). The data that support the findings of this pilot study are available from the corresponding author upon reasonable request.

Preprocedural 3DCT

In the intervention group, all patients underwent a cardiac coronary CT scan between 30 days and 1 week before PCI. Patients with a heart rate >65 bpm were prescribed a single dose of bisoprolol 5 mg to optimize imaging and reduce radiation exposure. All patients received a tablet of isosorbide nitrate sublingual 5 mg before scanning. Patients were scanned in flash mode with the ideal requirements of a pixel size <0.5 mm, slice thickness <0.8 mm, and slice increment <0.5 mm on SOMATOM Force CT scanner (Siemens Healthineers, Erlangen, Germany). Ultravist-370 was used as a contrast medium and dosed per protocol according to weight. If during the CT scan the heart rate remained >65 bpm, intravenous metoprolol was administered to lower the heart rate.

The CT images were analyzed and 3D reconstructed using the Mimics Innovation Suite software by Materialise (Leuven, Belgium). First, an accurate 3D reconstruction of the aorta and coronary arteries in the diastolic phase was obtained by applying the artifical intelligence-based automatic CT Heart tool in Mimics. The calcium was segmented using a simple thresholding operation (Figure 1A). Second, based on these 3D reconstructions, the MLA (mm²) and calcium arc (°) were obtained (Figure 1B). Next, the centerline of the aorta and coronary

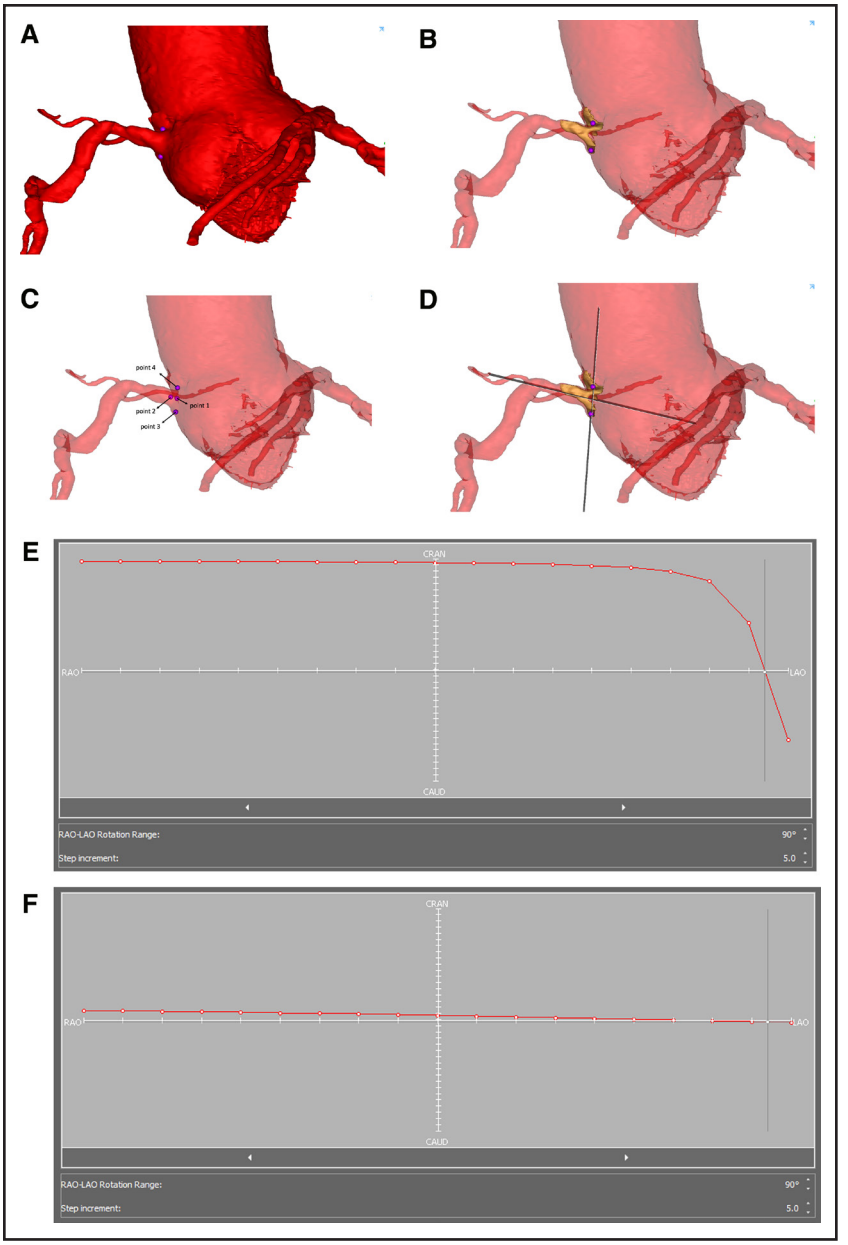

Figure 1. Three-dimensional (3D) computed tomography analysis. A 3D reconstruction of the aorta and right coronary artery (**A**). Calcium segmentation (**B**). The determination of 4 auxiliary points at the ostium (**C**). The creation of 2 perpendicular planes (**D**). The 2 S-curves of the planes that define the C-arm angle (**E** and **F**).

arteries was automatically calculated using the Fit Centerline tool. Based on this, the best-fit diameter (mm) was calculated at multiple locations along the coronary artery, giving an indication of a possible minimum stent diameter that could be a good fit. In addition, the distance (mm) along the centerline from the ostium to the end of arterial stenosis was calculated, giving an indication of a possible minimum stent length to use.

Finally, the optimal angle of the C-arm was determined to provide the frontal perpendicular view of the RCA ostium. To obtain this C-arm angle, 4 auxiliary points were indicated to create 2 planes. The 4 auxiliary points were defined as follows: point 1 is the ostium (at the cross-section of the centerline and the ostium), point 2 is near the ostium (taken at 3 mm from the ostium on the centerline), point 3 is located at the bottom of the coronary artery, where the cusp of the aortic valve starts, and point 4 is located right above the cusps, where the aorta starts to become wider. Next, the first plane along the RCA sagittal was defined by points 1, 2, and 3, and the second plane RCA cross-section crossed points 3 and 4 and was perpendicular to the first plane (Figure 1C). These 2 planes were taken as input for the Fluoroscopy tool in Mimics (Figure 1D). In this tool, the S curve of a plane visualizes all the C-arm angles for which the plane is seen as a line, in other words, a perpendicular view on that plane. The cross-section of the S curves of each of those planes results in the C-arm angle that gives a perpendicular view of both planes at the same time. This ultimately leads to the optimal C-arm angle. However, not every patient has a perfect cross-section of the S curves; in some rare occasions, there was no cross-section or the results were inoperable angles for the C-arm. In such cases a third plane along the RCA axial, perpendicular to the other 2 planes, was created. The cross-section of the S curves of this plane with each of the 2 original planes was defined, resulting in an alternative C-arm angle (Figure 1E and 1F; Video S1).

The CT scans of the intervention group were also reconstructed in 3mensio (Pie Medical Imaging) to compare the

Materialise C-arm angles with more commercially available software. On the short-axis image, the ostium of the RCA was located, and the line was rotated to cut through the center of the ostium of the RCA. The orthogonal view was given in the opposite image. In the angiography simulation view and 3D volume view, the C-arm angles were reproduced.

Intervention

In the control group, the C-arm angle was defined after contrast injections by fluoroscopy or cineangiography from ≥1 angles to the operator's satisfaction. In the intervention group, only in selected cases where it turned out that the aorto-ostial angle was not clearly visualized in the suggested working view, the operator was allowed to rotate the C-arm. An intravascular ultrasound (IVUS; OPTICROSS HD, 60 MHz; Boston Scientific) was performed by routine practice (pre-PCI IVUS) with an automatic pullback speed of 0.5 mm/s. When the IVUS was unable to cross the lesion, predilatation with a small balloon was allowed. After IVUS-guided calcium modification, stenting and postdilatation were performed as per routine practice. Stent diameter and length were determined by IVUS in both groups. Simultaneous IVUS during stent placement, the Szabo technique, or the use of an ostium locator were not allowed during stent implantation. When the operator was satisfied with the angiographic result, a final IVUS (post-PCI IVUS) was obtained, and these images were used for the primary end point. Additional interventions, such as additional stenting (if the ostium was not fully covered with struts) or postdilatation (in case of underexpansion or malapposition), were allowed. In these cases, a final clinical post-PCI IVUS run was obtained (Figure S1).

Trial End Points

IVUS images were analyzed offline by the core laboratory blinded to treatment allocation. The primary end point was the percentage of patients without geographic mismatch, defined as a fully covered ostium and a maximal length between the aorto-ostial junction and the most proximal protruding stent strut of no more than 3 mm (Figure S2). Secondary end points included the percentage of patients who need an additional stent after the final IVUS, the volume of contrast administered (milliliter), procedural radiation dose (milligray), and procedural duration (minute). Calcium arc, MLA (square millimeter), and stent diameter as predicted by 3DCT were correlated with IVUS-based measurements. Major adverse cardiac event defined as a composite of death, nonfatal myocardial infarction, nonfatal stroke, stent thrombosis, and target lesion failure was evaluated at 6 months (Figure S3).

Statistical Analysis

As there are no previous studies on topic that would allow a sample size calculation, we believe that 30 patients would be sufficient to show an effect and generate sufficient data for a power analysis to design a powered randomized controlled trial. Continuous data will be presented by treatment group using mean/SD (if normally distributed) or median/interquartile range (if not normally distributed). Categorical data will be presented using the observed frequencies and percentages. Continuous end points will be analyzed by Student *t* tests (if normally distributed) or by Mann-Whitney *U* test (if not normally distributed). Categorical end points will be analyzed by χ^2 tests, and odds ratios (+95% CI) will be calculated.

The agreement of calcium arc, MLA, and vessel diameter between 3DCT and IVUS will be presented using Pearson correlation coefficients and Bland-Altman analysis.

The C-arm angles determined by Materialise and 3mensio were compared in a Bland-Altman analysis, stratified by LAO/RAO (right anterior oblique) and CRA/CAU (caudal) views.

All statistical analyses were performed using SPSS 25.0 (SPSS-PC, Chicago, IL). *P* values of <0.05 were considered statistically significant.

RESULTS

Between January 2022 and February 2023, a total of 30 patients underwent randomization, equally distributed between both groups. Baseline prerandomization characteristics were well balanced between the groups (Table 1).

Three-Dimensional CT

The mean heart rate during 3DCT was 64±4 bpm. Two patients were in atrial fibrillation during the scan. The mean contrast dose was 73±29 mL. One patient had a coronary CT combined with a CT for transcatheter aortic valve implantation, for which a total of 75 mL of contrast was used, and 1 patient had to be scanned twice because of motion artifacts, requiring a total contrast dose of 170 mL. The median radiation dose during CT was 2.46 (1.34–4.65) mSv.

Table 1. Patient Characteristics

	Intervention group (n=15)	Control group (n=15)	*P* value
Age, y	69.6±10.4	72.4±10.2	0.5
Men, n (%)	13 (86.7)	8 (53.3)	0.05
Mean BMI	26.7±5.2	27.6±4.7	0.64
Diabetes, n (%)	1 (6.7)	4 (26.7)	0.15
Chronic kidney disease (eGFR <60 mL/min per 1.73 m²), n (%)	4 (26.7)	3 (20)	0.67
Peripheral artery disease, n (%)	2 (13.3)	1 (6.7)	0.37
Previous PCI, n (%)	3 (20.0)	3 (20.0)	1.00
Previous CABG, n (%)	5 (33.3)	0 (0)	0.01
Severe aortic stenosis present, %	1 (6.7)	2 (13.3)	0.56
Indication for coronary angiography			
Angina	8	4	0.14
Unstable angina	0	2	0.16
Cardiomyopathy	2	1	0.54
Silent ischemia	3	3	1.00
Preoperative	1	2	0.54
Other	1	3	0.28

BMI indicates body mass index; CABG, coronary artery bypass graft; eGFR, estimated glomerular filtration rate; and PCI, percutaneous coronary intervention.

Table 2. Lesion and Procedural Characteristics

	Intervention group (n=15)	Control group (n=15)	*P* value
Access site			
Radial	13	15	
Femoral	2	0	
Angiographic stenosis ostial RCA, %			
>90	6	5	
70–90	9	9	
50–70	0	1	
SYNTAX score 1	9.0 (5–12.5)	10 (5–13)	0.90
IVUS measurements pre-stenting			
MLA, mm^2 (n=14 in both groups)	3.97±1.85	3.76±1.58	0.75
Calcium arc, °	270 (85–270)	180 (90–270)	0.77
Lesion length, mm	13.78±7.82	18.62±14.42	0.27
Diameter distal artery, mm	4.22±0.64	4.35±0.53	0.54
Predilatation performed (number of patients)	12	15	
Total number of inflations predilatation	3 (2–5.5)	4 (3.5–6)	
Balloons used for predilatation			
Semicompliant balloon	1	2	
Noncompliant balloon	13	13	
Cutting balloon	3	3	
Scoring balloon	1	1	
IVL	1	2	
Rotational atherectomy (number of patients)	1	2*	
1.5 burr used	1	1	
1.75 burr used	0	1	
2.0 burr used	0	1	
Rotational atherectomy performed pre-IVUS	1	1	
Total number of stents placed in RCA			
1	14	12	
2	1	3	
Mean stent diameter implanted, mm	3.8±0.5	4.1±0.6	0.32
Mean stent length implanted, mm	30.4±11.6	27.3±7.7	0.40
Postdilatation performed pre-IVUS	7	7	
Extra postdilatation post-IVUS	3	4	
Underexpansion	3	2	
Other	0	2	
Periprocedural complications	1	0	

IVL indicates intravascular lithotripsy; IVUS, intravascular ultrasound; MLA, minimal lumen area; RCA, right coronary artery; and SYNTAX, Synergy Between Percutaneous Coronary Intervention With Taxus and Cardiac Surgery.

*In 1 patient, a 1.5 and 2.0 burr was used.

Procedural Characteristics

Procedural characteristics are shown in Table 2.

There was important patient heterogeneity considering the optimal angle for stent implantation (Figure 2). In general, more extreme LAO angles were used in the intervention group compared with the control group (61.47±13.41 versus 34.67±9.18; $P \leq 0.0001$).

In 2 patients (1 in each group), it was not possible to cross the ostial lesion with the IVUS catheter or with small balloons so rotational atherectomy was used for debulking. These patients were excluded from the analysis for MLA by IVUS, as calcium cracks might overestimate the true MLA. The median calcium arc was 270 (85–270) degrees, and the mean MLA was 3.97±1.85 mm^2 by IVUS.

Study End Points

While stent implantation was in the optimal position in all patients randomized to the intervention group, geographic mismatch was present in 5 (33%) patients randomized to the control group (P=0.06; Table 3; Figure 3). In addition to 3 patients with excessive aortic protrusion,

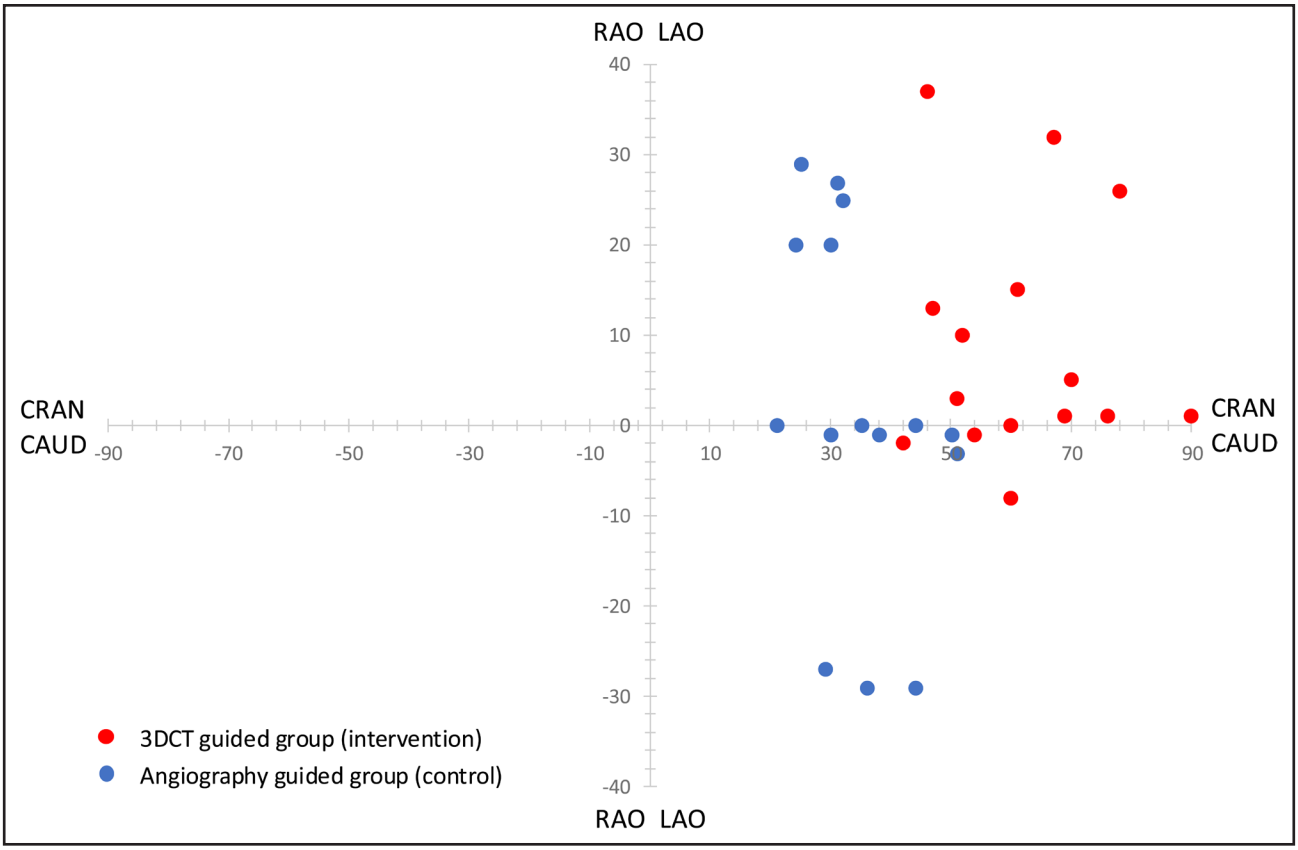

Figure 2. Working view angles during percutaneous coronary intervention.
Red, intervention group. Blue, control group. 3DCT indicates 3-dimensional computed tomography; CAUD, caudal; CRAN, cranial; LAO, left anterior oblique; and RAO, right anterior oblique.

the ostium was not covered in 2 patients randomized to the control group. An additional stent was implanted in 1 of these patients based on the post-PCI IVUS showing a 4.5-mm uncovered zone.

In an exploratory post hoc analysis, the percentage of patients with stent implantation within 1 mm of the ostium was significantly higher in patients randomized to the intervention group (11/15 [73%] versus 5/15 [33%]; *P*=0.03; Figure 3).

The mean amount of procedural contrast agent used (60.7±21.5 versus 116.7±37.5 mL; *P*≤0.0001), the mean procedural radiation dose (251.9 [195.6–393.32] versus 487.3 [407.4–634.00] mGy; *P*=0.03), the median procedure time (37 [24–42] versus 50 [42.5–67.5] minutes; *P*=0.03), and the median number of cine acquisitions performed before starting lesion preparation (1 [1–1] versus 4 [2–5]; *P*=0.0002) were significantly lower in patients randomized to the intervention group. The total amount of contrast used during CT scanning and PCI was equal among both groups (134±27.7 versus 116.7±37.5 mL; *P*=0.08; Table 3).

Stent expansion was excellent in the overall cohort without significant differences between the groups. The major adverse cardiac event rate at 6 months was 0% in the intervention group and 6.7% (1/15) in the control group (*P*=0.16). The patient in the control group died 76 days after PCI with unknown cause. This was graded as a possible event of stent thrombosis.

Table 3. Primary and Secondary End Points

	Intervention group (n=15)	Control group (n=15)	*P* value
% Patients without geographic mismatch	100 (15/15)	67.7 (10/15)	0.06
% Patients additional stent needed	0 (0/15)	6.7 (1/15)	0.49
Volume of contrast administered during PCI, mL	60.7±21.5	116.7±37.5	<0.0001
Total volume of contrast administered, mL	134±27.7	116.7±37.5	0.08
Procedural radiation dose, mGy	251.9 (195.6–393.3)	487.3 (407.4–634.0)	0.026
Procedural duration, min	30.0 (20.0–45.0)	50.0 (40.0–70.0)	0.009
Stent expansion, %	0.87±0.13	0.88±0.14	0.77
Median number of cine acquisitions before lesion preparation	1 (1–1)	4 (2–5)	0.0002
MACE at 6 mo	0/15	1/15	0.16

MACE indicates major adverse cardiac events; and PCI, percutaneous coronary intervention.

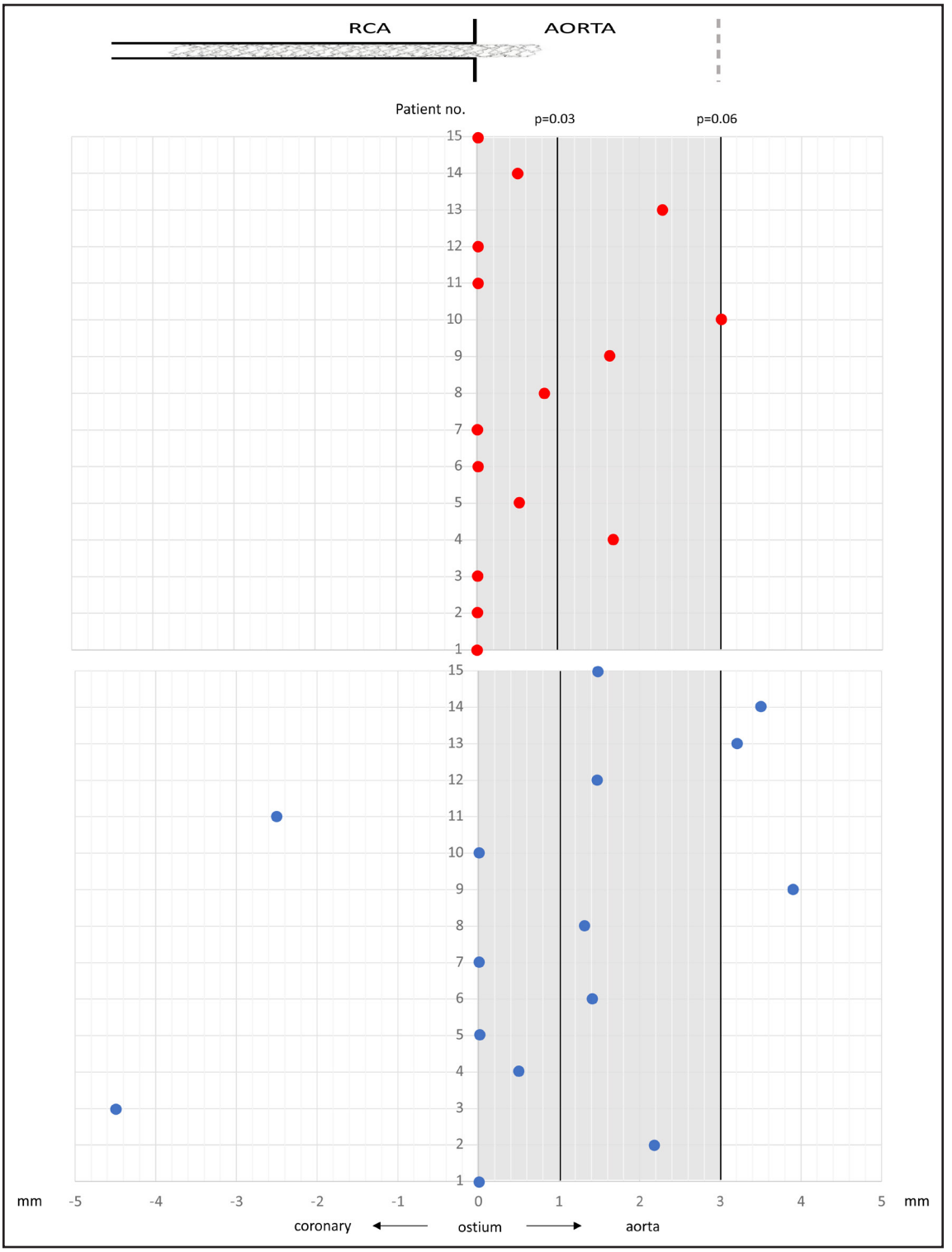

Figure 3. Primary end point.
Red, intervention group. Blue, control group. The dark gray zone represents 1 mm of stent protrusion in the aorta (11/15 [73%] vs 5/15 [33%]; *P*=0.03). The light gray zone represents 3 mm of stent protrusion in the aorta (4/15 [26%] vs 10/15 [67%]; *P*=0.06). RCA indicates right coronary artery.

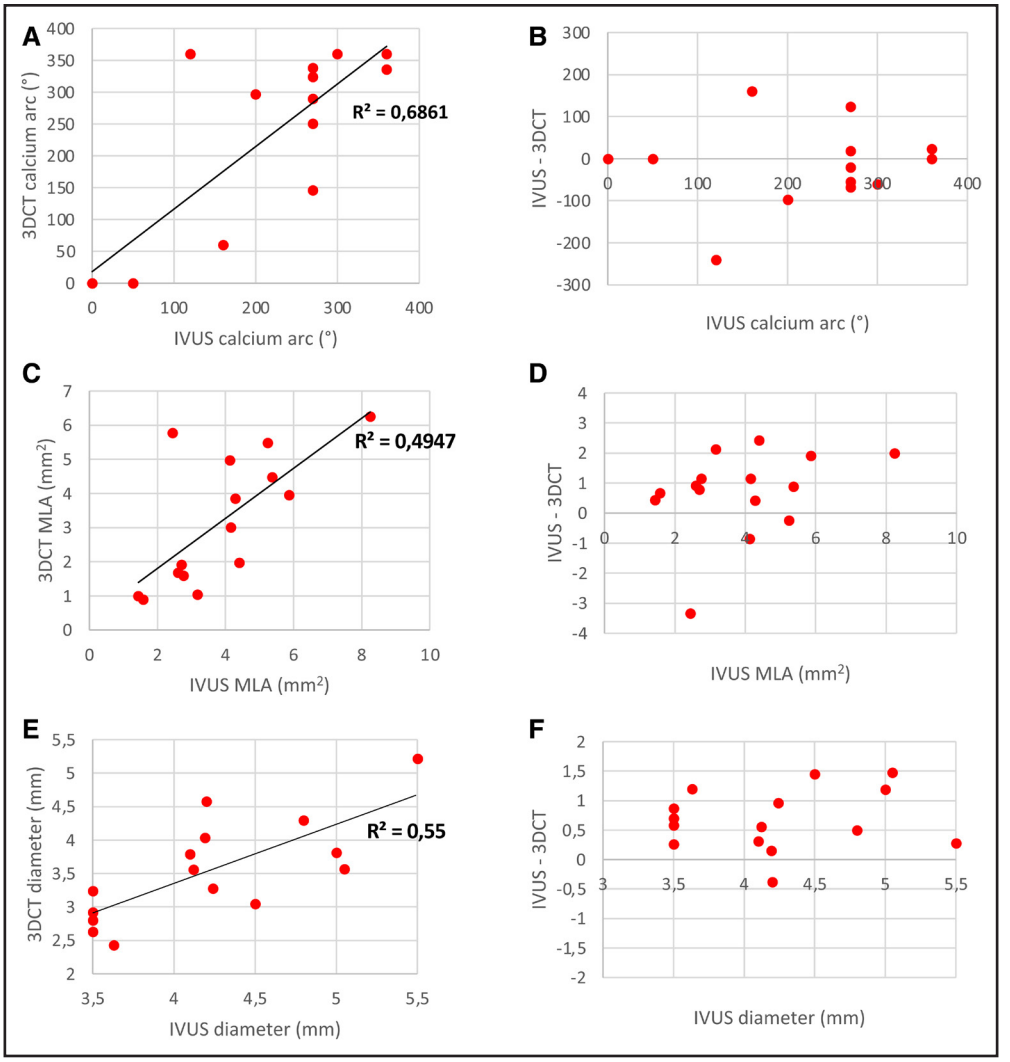

Figure 4. Three-dimensional computed tomography (3DCT) vs intravascular ultrasound (IVUS).
Correlation and Bland-Altman curves for calcium arc (**A** and **B**), minimal lumen area (MLA; **C** and **D**), and vessel diameter (**E** and **F**).

Lesion Characteristics

The calcium arc (R^2=0.69; P<0.0001), MLA (R^2=0.49; P<0.003), and vessel diameter (R^2=0.55; P<0.0001) were highly correlated between 3DCT and IVUS (Figure 4). However, Bland-Altman analysis showed a 12% vessel diameter undersizing with 3DCT compared with IVUS.

Comparison With Commercially Available Software

The comparison of the LAO/RAO and CRA/CAU angle views showed good correlation between Materialise and 3mensio (Figure S4).

DISCUSSION

This is the first randomized controlled trial to show the added value of 3DCT for preprocedural planning for PCI of aorto-ostial RCA lesions. Preprocedural 3DCT planning allowed for accurate imaging of the aorto-ostial plane and adequate assessment of lesion calcification, thereby allowing optimal stent positioning while reducing procedure time, contrast, and radiation.

Often encountered as the Achilles heel of interventional cardiology, the rate of TLR in PCI of aorto-ostial RCA lesions remains 14.2% at 3 years, even with the use of second-generation drug-eluting stents.[6] In previous retrospective studies, the main drivers for TLR of aorto-ostial lesions were stent underexpansion and geographic mismatch. The latter was present in 54% of patients and resulted in a 3-fold increase in the rate of TLR.[15] While the incidence of geographic mismatch in patients randomized to the control group was in line with these retrospective data (33% with a 3-mm and 66% with a 1-mm tolerance zone), stent implantation was within the predefined 3 mm tolerance zone in all patients randomized to preprocedural 3DCT planning. At 6-month follow-up, no significant difference in major adverse cardiac events was observed in our study, although 1 patient

in the control group had an unexplained death 76 days after PCI. An adequately powered future randomized trial is necessary to investigate whether preprocedural 3DCT can avoid geographic mismatch and effectively reduce TLR rates in these vulnerable patients.

In line with a previous retrospective CT study suggesting an average optimal viewing angle for PCI of aorto-ostial RCA lesions of LAO 79°/CRA 41°,[17] the average angle in our study was LAO 61°/CRA 13°. Retrospective studies revealed that a significant amount of unrecognized vessel foreshortening occurs in the working views selected by experienced interventional cardiologists.[17,18] The average viewing angle in our angio-guided group was found to be LAO 35°/CRA 9°, suggesting that interventionalists should use more extreme LAO angles in the majority of patients. However, every patient has a unique anatomy of the aorto-coronary junction defined by the origin of the RCA, the take-off angle from the aorta, and the rotation of the aortic root. This resulted in significant patient heterogeneity considering the optimal angle for stent implantation, thereby underscoring the potential benefit of individualized preprocedural CT planning. An integrated 3DCT linked with the angiography system in the catheterization laboratory could allow operators to virtually rotate the aorto-coronary junction to determine the optimal C-arm viewing angle in real time.[19,20] Cardiac motion and the patient's position on the catheterization laboratory table relative to the CT table seem to have little impact on the precision of 3DCT to define optimal fluoroscopic viewing angle.[17] Upfront determination of the optimal viewing angle allowed for 1 single setup shot before starting lesion preparation in 13 of 15 (87%) patients, while a median of 4 shots were deemed necessary in patients randomized to the angio-guided arm. This resulted in a 48% reduction in procedural contrast, radiation dose, and procedure times that were on average 13 minutes shorter. Prediction of the C-arm angle has been long established in transcatheter aortic valve implantation procedures, with a decrease in the number of aortograms, shortening of procedure time, and reduction in the use of contrast agents.[21,22] Commercially available software to analyze the optimal C-arm angulation in transcatheter aortic valve implantation procedures can be a good alternative to Materialise software to determine the optimal C-arm angle in PCI of the ostium of the RCA.

Alternative techniques have been described to optimize stent positioning at the level of the RCA ostium. Some operators use a second guidewire in the aorta just below the ostium to prevent deep intubation of the guiding and to define a landmark for stent placement at the level of the ostium. Although cheap and frequently used, this floating wire technique is poorly studied, and the risk of vessel foreshortening in a 2-dimensional projection cannot be excluded. Szabo et al[23] described a technique for precise positioning of an aorto-ostial stent by using a floating guidewire positioned through the proximal stent strut to anchor the stent at the ostial location. Its usefulness has been demonstrated in larger case series with IVUS documentation of correct positioning.[24] The Ostial-PRO stent positioning system is a guide extension with self-expandable radioopaque nitinol feet at the tip to mark the plane of the aortic wall. This simple device proved successful for optimal positioning in all 30 cases reported in a pilot study.[25] Finally, some operators use live IVUS with the probe on a buddy wire to have real-time imaging during the initial partial inflation of the stent. Importantly, the use of all mentioned techniques was not allowed in our study.

In accordance with previous studies, 3DCT was able to predict IVUS lesion characteristics such as the calcium arc and MLA.[26–28] However, in our data, CT angiography showed a systematic undersizing of the predicted vessel diameter by 12% compared with IVUS, likely explained by scattering from surrounding calcium. Upfront CT-based determination of the calcium modification strategy may allow for further shortening of the duration of the procedure because devices such as rotablator atherectomy or shockwave balloons can already be prepared by nursing staff during the positioning of the guiding and wiring of the vessel.

Although the risk of bias was limited because the primary end point was adjudicated by a blinded core laboratory, our study was limited by its open-label single-center design and the sample size. Therefore, we consider our results to be hypothesis generating. Performing an upfront 3DCT and offline preprocedural planning has potential limitations in terms of health care costs, patient radiation and contrast doses, and patient comfort, as PCI had to be performed in a second staged procedure. However, in an increasing number of patients, the indication for invasive angiography is based on CT angiography or CT transcatheter aortic valve implantation. In our study, offline preprocedural planning could be performed without additional scanning in 4 of 15 patients. Moreover, the reduction in procedural contrast use offsets the amount of additional contrast necessary for the CT scan, rendering the total amount of contrast equal between the groups. Finally, we did not perform a CT with measurement of fractional flow reserve, and preprocedural planning could be completed by including functional evaluation and prediction of post-PCI fractional flow reserve.

CONCLUSIONS

Preprocedural 3DCT planning for PCI of aorto-ostial RCA lesions allows for optimal stent positioning while reducing procedure time, contrast, and radiation dose.

ARTICLE INFORMATION

Received September 21, 2023; accepted December 16, 2024.

Affiliations

Department of Cardiology, Ziekenhuis Oost-Limburg, Genk, Belgium (D.M.F.v.d.B., E.M.P., E.W., D.C., E.M., B.F., M.V., J.D., K.A.). Materialise HQ, Leuven, Belgium (K.D., K.D.L.). Faculty of Medicine and Life Sciences, University Hasselt, Diepenbeek, Belgium (E.M., J.D., K.A.).

Sources of Funding

None.

Disclosures

Dr Dens has consultancy contracts with Abbott, Boston Scientific, Interventional Medical Device Solutions, Medtronic Terumo, and TOP Medical (a distributor for Asahi). The other authors report no conflicts.

Supplemental Material

Figures S1–S4
Video S1

REFERENCES

1. Levi Y, Kobo O, Halabi M, Al Haddad I, Chevalier B, Polad J, Laanmets P, Witkowski A, Monsegu J, Iniguez AR, Mamas MA, Roguin A. Treatment of ostial right coronary artery narrowings: outcomes from the multicenter prospective e-ULTIMASTER registry. *J Soc Cardiovasc Angiogr Interv*. 2023;2:100604. doi: 10.1016/j.jscai.2023.100604
2. Mavromatis K, Ghazzal Z, Veledar E, Diamandopoulos L, Weintraub WS, Douglas JS, Kalynych AM. Comparison of outcomes of percutaneous coronary intervention of ostial versus nonostial narrowing of the major epicardial coronary arteries. *Am J Cardiol*. 2004;94:583–587. doi: 10.1016/j.amjcard.2004.05.020
3. Freeman M, Clark DJ, Andrianopoulos N, Duffy SJ, Lim HS, Brennan A, Charter K, Shaw J, Horrigan M, Ajani AE, et al; Melbourne Interventional Group. Outcomes after percutaneous coronary intervention of ostial lesions in the era of drug-eluting stents. *Catheter Cardiovasc Interv*. 2009;73:763–768. doi: 10.1002/ccd.21941
4. Luz A, Hughes C, Magalhães R, Bisceglia T, Descoutures F, Tamamm K, Tchetche D, Sauguet A, Farah B, Fajadet J. Stent implantation in aorto-ostial lesions: long-term follow-up and predictors of outcome. *EuroIntervention*. 2012;7:1069–1076. doi: 10.4244/EIJV7I9A170
5. Patel Y, Depta JP, Patel JS, Masrani SK, Novak E, Zajarias A, Kurz HI, Lasala JM, Bach RG, Singh J. Impact of intravascular ultrasound on the long-term clinical outcomes in the treatment of coronary ostial lesions. *Catheter Cardiovasc Interv*. 2016;87:232–240. doi: 10.1002/ccd.25034
6. Mitomo S, Jabbour RJ, Watanabe Y, Mangieri A, Ancona M, Regazzoli D, Tanaka A, Nakajima A, Naganuma T, Giannini F, et al. Comparison of mid-term clinical outcomes after treatment of ostial right coronary artery lesions with early and new generation drug-eluting stents: insights from an international multicenter registry. *Int J Cardiol*. 2018;254:53–58. doi: 10.1016/j.ijcard.2017.10.066
7. Iakovou I, Ge L, Michev I, Sangiorgi GM, Montorfano M, Airoldi F, Chieffo A, Stankovic G, Vitrella G, Carlino M, et al. Clinical and angiographic outcome after sirolimus-eluting stent implantation in aorto-ostial lesions. *J Am Coll Cardiol*. 2004;44:967–971. doi: 10.1016/j.jacc.2004.05.058
8. Al-Lamee R, Ielasi A, Latib A, Godino C, Mussardo M, Arioli F, Figini F, Piraino D, Carlino M, Montorfano M, et al. Comparison of long-term clinical and angiographic outcomes following implantation of bare metal stents and drug-eluting stents in aorto-ostial lesions. *Am J Cardiol*. 2011;108:1055–1060. doi: 10.1016/j.amjcard.2011.06.004
9. Sugihara R, Ueda Y, Nishimoto Y, Takahashi K, Murakami A, Ueno K, Takeda Y, Hirata A, Kashiwase K, Higuchi Y, et al. Outcomes of first- versus second-generation drug-eluting stent implanted for right coronary artery ostial narrowing. *Am J Cardiol*. 2017;119:852–855. doi: 10.1016/j.amjcard.2016.11.038
10. De Rosa M, Santulli G. Effectiveness of new generation drug-eluting stents in ostial right coronary artery lesions. *Int J Cardiol*. 2018;254:84–86. doi: 10.1016/j.ijcard.2017.11.105
11. Aviram G, Shmilovich H, Finkelstein A, Rosen G, Banai S, Graif M, Keren G. Coronary ostium-straight tube or funnel-shaped? A computerized tomographic coronary angiography study. *Acute Card Care*. 2006;8:224–228. doi: 10.1080/17482940601026519
12. Malaiapan Y, Leung M, White AJ. The role of intravascular ultrasound in percutaneous coronary intervention of complex coronary lesions. *Cardiovasc Diagn Ther*. 2020;10:1371–1388. doi: 10.21037/cdt-20-189
13. Zhang M, Matsumura M, Usui E, Noguchi M, Fujimura T, Fall KN, Zhang Z, Nazif TM, Parikh SA, Rabbani LE, et al. Intravascular ultrasound-derived calcium score to predict stent expansion in severely calcified lesions. *Circ Cardiovasc Interv*. 2021;14:e010296. doi: 10.1161/CIRCINTERVENTIONS.120.010296
14. Rubinshtein R, Ben-Dov N, Halon DA, Lavi I, Finkelstein A, Lewis BS, Jaffe R. Geographic miss with aorto-ostial coronary stent implantation: insights from high-resolution coronary computed tomography angiography. *EuroIntervention*. 2015;11:301–307. doi: 10.4244/EIJV11I3A57
15. Dishmon DA, Elhaddi A, Packard K, Gupta V, Fischell TA. High incidence of inaccurate stent placement in the treatment of coronary aorto-ostial disease. *J Invasive Cardiol*. 2011;23:322–326.
16. Abhyankar A, Gai L, Bailey BP. Angioplasty through a stent side door. *Int J Cardiol*. 1996;55:107–110. doi: 10.1016/0167-5273(96)02621-6
17. Kočka V, Thériault-Lauzier P, Xiong TY, Ben-Shoshan J, Petr R, Laboš M, Buithieu J, Mousavi N, Pilgrim T, Praz F, et al. Optimal fluoroscopic projections of coronary ostia and bifurcations defined by computed tomographic coronary angiography. *JACC Cardiovasc Interv*. 2020;13:2560–2570. doi: 10.1016/j.jcin.2020.06.042
18. Green NE, Chen SY, Hansgen AR, Messenger JC, Groves BM, Carroll JD. Angiographic views used for percutaneous coronary interventions: a three-dimensional analysis of physician-determined vs. computer-generated views. *Catheter Cardiovasc Interv*. 2005;64:451–459. doi: 10.1002/ccd.20331
19. Wink O, Hecht HS, Ruijters D. Coronary computed tomographic angiography in the cardiac catheterization laboratory: current applications and future developments. *Cardiol Clin*. 2009;27:513–529. doi: 10.1016/j.ccl.2009.04.002
20. Collet C, Sonck J, Leipsic J, Monizzi G, Buytaert D, Kitslaar P, Andreini D, De Bruyne B. Implementing coronary computed tomography angiography in the catheterization laboratory. *JACC Cardiovasc Imaging*. 2021;14:1846–1855. doi: 10.1016/j.jcmg.2020.07.048
21. Blanke P, Weir-McCall JR, Achenbach S, Delgado V, Hausleiter J, Jilaihawi H, Marwan M, Norgaard BL, Piazza N, Schoenhagen P, et al. Computed tomography imaging in the context of transcatheter aortic valve implantation (TAVI)/transcatheter aortic valve replacement (TAVR): an expert consensus document of the Society of Cardiovascular Computed Tomography. *J Cardiovasc Comput Tomogr*. 2019;13:1–20. doi: 10.1016/j.jcct.2018.11.008
22. Mehier B, Dubourg B, Eltchaninoff H, Durand E, Tron C, Cribier A, Michelin P, Dacher JN. MDCT planning of transcatheter aortic valve implantation (TAVI): determination of optimal C-arm angulation. *Int J Cardiovasc Imaging*. 2020;36:1551–1557. doi: 10.1007/s10554-020-01846-0
23. Szabo S, Abramowitz B, Vaitkus PT. New technique for aorto-ostial stent placement. *Am J Cardiol*. 2005;96:212H.
24. Kern MJ, Ouellette D, Frianeza T. A new technique to anchor stents for exact placement in ostial stenoses: the stent tail wire or Szabo technique. *Catheter Cardiovasc Interv*. 2006;68:901–906. doi: 10.1002/ccd.20613
25. Fischell TA, Saltiel FS, Foster MT, Wong SC, Dishman DA, Moses J. Initial clinical experience using an ostial stent positioning system (Ostial Pro) for the accurate placement of stents in the treatment of coronary aorto-ostial lesions. *J Invasive Cardiol*. 2009;21:53–59.
26. Fischer C, Hulten E, Belur P, Smith R, Voros S, Villines TC. Coronary CT angiography versus intravascular ultrasound for estimation of coronary stenosis and atherosclerotic plaque burden: a meta-analysis. *J Cardiovasc Comput Tomogr*. 2013;7:256–266. doi: 10.1016/j.jcct.2013.08.006
27. Feuchtner G, Loureiro R, Bezerra H, Rocha-Filho JA, Sarwar A, Pflederer T, Marwan M, Petranovic M, Raffel CO, Brady TB, et al. Quantification of coronary stenosis by dual source computed tomography in patients: a comparative study with intravascular ultrasound and invasive angiography. *Eur J Radiol*. 2012;81:83–88. doi: 10.1016/j.ejrad.2010.12.008
28. Kass M, Glover CA, Labinaz M, So DY, Chen L, Yam Y, Chow BJ. Lesion characteristics and coronary stent selection with computed tomographic coronary angiography: a pilot investigation comparing CTA, QCA and IVUS. *J Invasive Cardiol*. 2010;22:328–334.